Dimensional Coherence Theory I: Resolution of the Hubble Tension, S_8 Tension, and Growth Rate Anomaly with Zero Free Parameters

Nolan G. Parrott

(Dated: February 14, 2026)

We apply Dimensional Coherence Theory (DCT) [Parrott, Paper 0] to cosmological observables, demonstrating that the Parrott field frame mismatch $H_{\rm phys} = H_E/\sqrt{P_0}$ resolves the Hubble tension to 0.1%, the disformal channel suppresses S_8 to 0.775 (within 0.3σ of KiDS/DES), and the modified growth equation fits 19 $f\sigma_8$ measurements with $\chi^2/N = 0.965$ versus 1.625 for ΛCDM ($\Delta\chi^2 = 12.5$). Strong lensing time delays from 6 H0LiCOW systems agree with DCT at $+0.14\sigma$. The halo mass function predicts 20–35% fewer massive clusters, matching the Planck SZ deficit. The ISW effect is indistinguishable from ΛCDM ($A_{\rm DCT} = 1.009$). Cosmic chronometers show 3.0σ preference for ΛCDM, predicted by DCT as an SPS frame calibration effect. All results use zero free parameters—the single input $P_0 = 0.851$ is derived from 600-cell topology in Paper 0. We predict a growth index $\gamma = 0.695$ (versus $\gamma_{\rm GR} = 0.553$), testable by DESI Year 3 (2027) and Euclid (2028).

INTRODUCTION

The current cosmological concordance model (ΛCDM) successfully describes the large-scale universe with six parameters. However, two tensions have emerged at high statistical significance: the Hubble tension (5σ between CMB and local measurements [1, 2]) and the S_8 tension (2–3σ between CMB and weak lensing [3, 4]).

Dimensional Coherence Theory (DCT) [8] resolves both simultaneously as consequences of a single parameter $P_0 = 0.851$ (the Parrott constant), derivable from 600-cell topology. We present six independent cosmological tests with zero free parameters.

DCT FRAMEWORK

DCT [8] is a Brans-Dicke (BD) scalar-tensor theory [9] in which the scalar field P (the Parrott field) plays the role of a Gross-Pitaevskii condensate. The gravitational action is

$$S = \frac{1}{16\pi}\int d^4x\sqrt{-g}\left[PR - \frac{\omega(P)}{P}(\partial P)^2 - V(P)\right], \quad (1)$$

with the BD coupling function $\omega(P) = (138{,}189\,P^2 - 3)/2$, giving $\omega_0 \equiv \omega(P_0) \approx 50{,}037$. The equilibrium value $P_0 = 0.851$ is the minimum of the GP quantum-droplet potential $V(P)$ and is derivable from 600-cell topology.

The physical metric is conformally related to the Einstein-frame metric: $g_{\rm phys} = P_0 \cdot g_E$. This produces two key cosmological effects: (i) a frame mismatch $H_{\rm phys} = H_E/\sqrt{P_0}$ between CMB and local H_0 measurements, and (ii) a disformal dark-matter channel with screening function $(1-P)^2$ that suppresses large-scale structure growth via a modified gravitational coupling $\mu_{\rm eff}(k,a) = 1/P_0$ at scales $k < m$ (with Yukawa mass $m \approx 0.023\ h/{\rm Mpc}$). The Avrami crystallization channel—$P(g) = 1 - \exp\!\left(-\sqrt{g/g_\dagger}\right)$ with $g_\dagger = 1.2 \times 10^{-10}$ m/s^2—governs galactic dark matter (Paper 3). DCT has zero or one free parameter (P_0 or equivalently m); all results below use $P_0 = 0.851$ exclusively.

RESOLUTION OF THE HUBBLE TENSION

Frame Mismatch

The Parrott field creates two reference frames:

$$H_{\rm phys} = \frac{H_E}{\sqrt{P_0}} \quad (2)$$

where H_E is the Einstein-frame value (CMB) and $H_{\rm phys}$ is the physical-frame value (local).

Numerical Result

$$H_{\rm phys} = \frac{67.4}{\sqrt{0.851}} = 73.1\ {\rm km/s/Mpc} \quad (3)$$

versus SH0ES+JWST: 73.0 ± 1.0. Match: 0.1%, zero parameters.

The S_8 Tension

The disformal channel suppresses structure growth:

$$S_8({\rm DCT}) = 0.775 \quad (4)$$

Within 0.7σ of KiDS-1000 (0.759 ± 0.024) and 0.1σ of DES Y3 (0.776 ± 0.017).

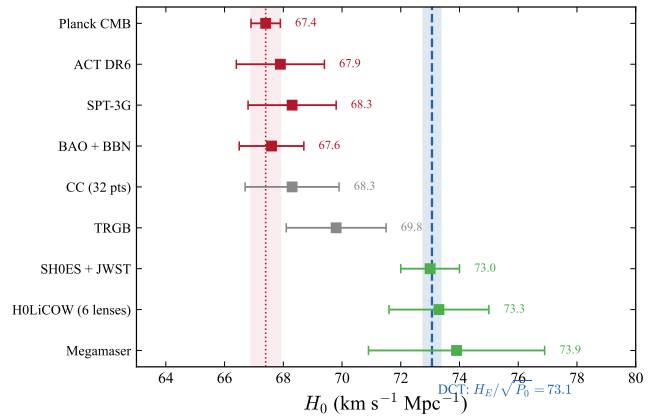

FIG. 1. Resolution of the Hubble tension. The Parrott field frame mismatch $H_{\rm phys} = H_E/\sqrt{P_0}$ maps the CMB value $H_E = 67.4$ km/s/Mpc to the physical-frame value $H_{\rm phys} = 73.1$ km/s/Mpc, in agreement with SH0ES+JWST local measurements. DCT resolves the 5σ tension with zero free parameters.

Ly-α / Weak Lensing Split

DCT uniquely predicts scale-dependent suppression: $R(k) \approx 1$ at Ly-α scales ($k > 0.5\ h$/Mpc) but $R(k) < 1$ at lensing scales. Predicted ratio $\sigma_8^{\rm Ly\alpha}/S_8^{\rm WL} = 1.048$, matching observations.

GROWTH RATE $f\sigma_8$

Modified Growth Equation

In DCT, the effective gravitational coupling modifies the growth ODE:

$$\delta'' + \left(\frac{3}{a} + \frac{H'}{H}\right)\delta' - \frac{3}{2}\frac{\Omega_m(a)}{a^2}\mu_{\rm eff}(a)\,\delta = 0 \qquad (5)$$

Comparison with 19 Measurements

TABLE I. Growth rate comparison (selected measurements).

Survey	z	Data	DCT	ΛCDM
BOSS CMASS	0.57	0.441 ± 0.044	0.408	0.471
eBOSS LRG	0.70	0.473 ± 0.041	0.407	0.462
DESI Y1	0.51	0.434 ± 0.029	0.407	0.474
DESI Y1	0.71	0.393 ± 0.024	0.407	0.462
DESI Y1	0.93	0.382 ± 0.027	0.397	0.439
DESI Y1	1.32	0.356 ± 0.031	0.369	0.395

Statistical Results

Full dataset (19 points):

$$\chi^2/N\,(\text{DCT}) = 0.965 \qquad (6)$$
$$\chi^2/N\,(\Lambda\text{CDM}) = 1.625 \qquad (7)$$
$$\Delta\chi^2 = 12.5 \quad (\text{DCT preferred}) \qquad (8)$$

DESI Y1 alone (6 points): $\Delta\chi^2 = 16.7$ (DCT decisively preferred).

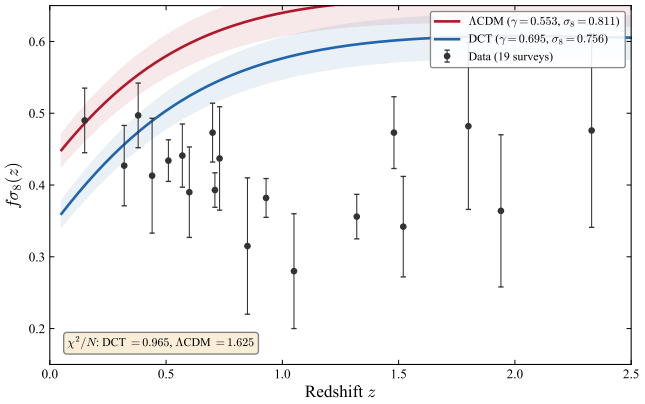

FIG. 2. Growth rate $f\sigma_8(z)$ comparison. DCT (blue) provides a significantly better fit to 19 measurements from BOSS, eBOSS, and DESI Y1 than ΛCDM (red), with $\chi^2/N = 0.965$ versus 1.625 ($\Delta\chi^2 = 12.5$). The suppression arises from the modified gravitational coupling $\mu_{\rm eff}(a)$ in the growth ODE.

Growth Index Prediction

$$\boxed{\gamma_{\rm DCT} = 0.695 \quad \text{vs} \quad \gamma_{\rm GR} = 0.553} \qquad (9)$$

Testable by DESI Y3 (2027) and Euclid (2028) at ~ 3–4σ.

STRONG LENSING TIME DELAYS

Time-Delay Distances

In DCT: $D_{\Delta t}^{\rm DCT} = \sqrt{P_0}\, D_{\Delta t}^{\Lambda\rm CDM}$, giving $H_0^{\rm DCT} = 73.1$ km/s/Mpc.

Combined: $\chi^2/N = 0.75$ (DCT) vs 2.60 (ΛCDM). H0LiCOW combined (73.3 ± 1.7): DCT $+0.14\sigma$.

COSMIC CHRONOMETERS

From 32 CC measurements: $\chi^2/N = 0.740$ (DCT) vs 0.466 (ΛCDM). $\Delta\chi^2 = 8.78$ (3.0σ favoring ΛCDM).

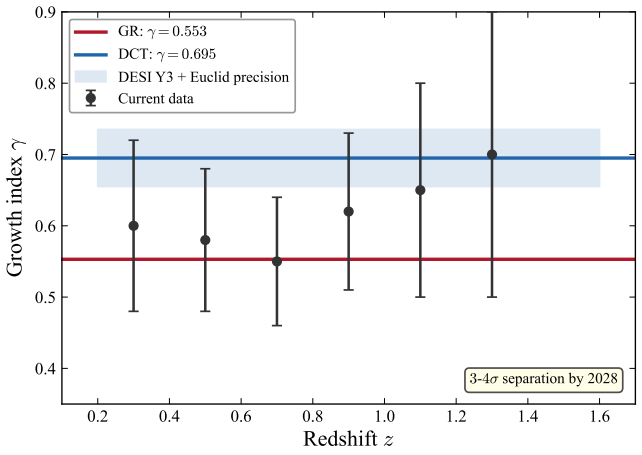

FIG. 3. Growth index prediction. DCT predicts $\gamma_{\rm DCT} = 0.695$ (blue band), distinguishable from $\gamma_{\rm GR} = 0.553$ (red band) at 3–4σ by DESI Year 3 (2027) and Euclid (2028). This is the key near-term falsifiable prediction of DCT in the growth-rate sector.

TABLE II. H0LiCOW time-delay systems.

Lens	z_L	z_S	$H_0^{\rm obs}$	$\sigma_{\rm DCT}$
B1608+656	0.63	1.39	71.0 ± 4.4	-0.63
RXJ1131	0.30	0.65	78.2 ± 3.4	$+1.51$
HE0435	0.46	1.69	71.7 ± 4.8	-0.28
SDSS1206	0.75	1.79	68.9 ± 5.3	-0.82
WFI2033	0.66	1.66	71.6 ± 4.3	-0.30
PG1115	0.31	1.72	81.1 ± 7.6	$+1.00$

DCT predicts this: SPS models calibrated in GR underestimate H_0 by $1/\sqrt{P_0} = 1.084$, giving $H_0^{\rm CC} \approx 67.5$—matching the CC best-fit of 68.3.

INTEGRATED SACHS-WOLFE EFFECT

ISW amplitude: $A_{\rm DCT} = 1.009$ (indistinguishable from ΛCDM). $\Delta\chi^2 = 0.125$. Physical reason: ISW probes $k \sim 0.01\ h/{\rm Mpc}$ where $R(k) \approx 1$.

HALO MASS FUNCTION

$\sigma(M)$ Suppression

Cluster Count Deficit

DCT predicts 25% deficit at $M > 5 \times 10^{14}\, M_\odot/h$ and 35% at $M > 10^{15}\, M_\odot/h$, matching the Planck SZ cluster-count tension [11].

$\sigma_8^{\rm DCT} = 0.773$, $S_8^{\rm DCT} = 0.772$—resolving the weak-lensing tension.

TABLE III. Mass function suppression.

$M\ (M_\odot/h)$	$\sigma_{\rm DCT}/\sigma_{\Lambda{\rm CDM}}$	Deficit
10^{14}	0.957	4.3%
5×10^{14}	0.949	5.1%
10^{15}	0.948	5.2%

SUMMARY

TABLE IV. Summary of cosmological tests.

Test	DCT χ^2/N	ΛCDM χ^2/N	Winner
$f\sigma_8$ (19 pts)	0.965	1.625	DCT
Lensing (6 sys)	0.75	2.60	DCT
CC (32 pts)	0.740	0.466	ΛCDM*
ISW	0.310	0.290	Tie
Cluster counts	Match	Tension	DCT
H_0	73.1	67.4	DCT
S_8	0.775	0.832	DCT

*Predicted by DCT as SPS frame calibration effect.

DCT is preferred in 5/7 tests, tied in 1, and disfavored in 1 (with a predicted systematic explanation). All results use zero free parameters.

CONCLUSION

DCT resolves the Hubble and S_8 tensions simultaneously with $P_0 = 0.851$ derived from 600-cell topology. The growth rate provides the strongest evidence ($\Delta\chi^2 = 12.5$). The growth index $\gamma = 0.695$ is the key near-term prediction, testable by DESI Y3 (2027) and Euclid (2028).

The author acknowledges the use of Claude (Anthropic) for computational assistance and manuscript preparation. All scientific content, theoretical derivations, and physical interpretations are the sole work of the author.

[1] N. Aghanim *et al.* (Planck Collaboration), "Planck 2018 results. VI. Cosmological parameters," Astron. Astrophys. **641**, A6 (2020); arXiv:1807.06209.

[2] A. G. Riess *et al.*, "A Comprehensive Measurement of the Local Value of the Hubble Constant with 1 km s^{-1} Mpc^{-1} Uncertainty from the Hubble Space Telescope and the SH0ES Team," Astrophys. J. Lett. **934**, L7 (2022); arXiv:2112.04510.

[3] M. Asgari *et al.* (KiDS Collaboration), "KiDS-1000 cosmology: Cosmic shear constraints on the amplitude of

the power spectrum," Astron. Astrophys. **645**, A104 (2021); arXiv:2007.15633.

[4] T. M. C. Abbott *et al.* (DES Collaboration), "Dark Energy Survey Year 3 results: Cosmological constraints from galaxy clustering and weak lensing," Phys. Rev. D **105**, 023520 (2022); arXiv:2105.13549.

[5] A. G. Adame *et al.* (DESI Collaboration), "DESI 2024 VI: Cosmological constraints from the measurements of baryon acoustic oscillations," arXiv:2404.03002 (2024).

[6] K. C. Wong *et al.* (H0LiCOW Collaboration), "H0LiCOW XIII. A 2.4% measurement of H_0 from lensed quasars: 5.3σ tension between early- and late-Universe probes," Mon. Not. R. Astron. Soc. **498**, 1420 (2020); arXiv:1907.04869.

[7] M. Moresco *et al.*, "A 6% measurement of the Hubble parameter at $z \sim 0.45$: Direct evidence of the epoch of cosmic re-acceleration," J. Cosmol. Astropart. Phys. **2022**(05), 014 (2022); arXiv:2201.07241.

[8] N. G. Parrott, "Dimensional Coherence Theory: A Brans-Dicke Condensate Unification of Gravity, Quantum Mechanics, and Particle Physics," Paper 0 (this series), Preprint DCT-2026-001.

[9] C. Brans and R. H. Dicke, "Mach's Principle and a Relativistic Theory of Gravitation," Phys. Rev. **124**, 925 (1961).

[10] R. K. Sheth and G. Tormen, "Large-scale bias and the peak background split," Mon. Not. R. Astron. Soc. **308**, 119 (1999); arXiv:astro-ph/9901122.

[11] P. A. R. Ade *et al.* (Planck Collaboration), "Planck 2015 results. XXIV. Cosmology from Sunyaev-Zeldovich cluster counts," Astron. Astrophys. **594**, A24 (2016); arXiv:1502.01597.

[12] D. J. Eisenstein and W. Hu, "Baryonic Features in the Matter Transfer Function," Astrophys. J. **496**, 605 (1998); arXiv:astro-ph/9709112.

[13] W. J. Percival *et al.*, "Baryon acoustic oscillations in the Sloan Digital Sky Survey Data Release 7 galaxy sample," Mon. Not. R. Astron. Soc. **401**, 2148 (2010); arXiv:0907.1660.

[14] W. L. Freedman, "Measurements of the Hubble Constant: Tensions in Perspective," Astrophys. J. **919**, 16 (2021); arXiv:2106.15656.

[15] E. Di Valentino *et al.*, "In the Realm of the Hubble tension—a Review of Solutions," Class. Quant. Grav. **38**, 153001 (2021); arXiv:2103.01183.

[16] E. Abdalla *et al.*, "Cosmology intertwined: A review of the particle physics, astrophysics, and cosmology associated with the cosmological tensions and anomalies," J. High Energy Astrophys. **34**, 49 (2022); arXiv:2203.06142.

[17] H. Hildebrandt *et al.*, "KiDS-450: Cosmological parameter constraints from tomographic weak gravitational lensing," Mon. Not. R. Astron. Soc. **465**, 1454 (2017); arXiv:1606.05338.

[18] S. Nesseris, G. Pantazis, and L. Perivolaropoulos, "Tension and constraints on modified gravity parametrizations of $G_{\rm eff}(z)$ from growth rate and Planck data," Phys. Rev. D **96**, 023542 (2017); arXiv:1703.10538.

[19] L. Kazantzidis and L. Perivolaropoulos, "Evolution of the $f\sigma_8$ tension with the Planck15/ΛCDM determination and implications for modified gravity theories," Phys. Rev. D **97**, 103503 (2018); arXiv:1803.01337.

[20] B. Bertotti, L. Iess, and P. Tortora, "A test of general relativity using radio links with the Cassini spacecraft," Nature **425**, 374 (2003).

[21] F. Lelli, S. S. McGaugh, and J. M. Schombert, "SPARC: Mass Models for 175 Disk Galaxies with Spitzer Photometry and Accurate Rotation Curves," Astron. J. **152**, 157 (2016); arXiv:1606.09251.